Available online at www.sciencedirect.com
ScienceDirect
Radiation Measurements 43 (2008) S588–S590
Radiation Measurements
www.elsevier.com/locate/radmeas

Surface energy gradient surfaces created by latent alpha-particle tracks in SSNTDs

W.Y. Li, K.N. Yu*

Department of Physics and Materials Science, City University of Hong Kong, Tat Chee Avenue, Kowloon Tong, Hong Kong

Abstract

Surface energy gradient surfaces with changes in the ratio of the polar component (γ_s^p) to the dispersive component (γ_s^d) of the surface energy γ_s have been successfully fabricated by irradiating CR-39 solid-state nuclear track detectors (SSNTDs) with 3 MeV alpha particles with different fluence followed by irradiation with ultraviolet photons with 257 nm. The alpha-particle source has an activity of 0.1 μCi and the irradiation time ranges from 1 to 7 d. The contact angles for doubly distilled water, glycerin and ethylene glycol, as well as γ_s do not vary significantly with the alpha-particle irradiation. In contrast, γ_s^p decreases steadily while γ_s^d increases steadily, and the ratio γ_s^p/γ_s^d decreases significantly with the alpha-particle fluence. Such surface energy gradient surfaces are of particular interest for establishing the relationship between the γ_s^p/γ_s^d ratio and the biocompatibility.

Keywords: CR-39; Alpha particle; Surface energy; Biocompatibility

1. Introduction

Researches on the biocompatibility of different substrates are important. For example, a key factor to the success of radiobiological experiments relies on the biocompatibility of the employed substrate. If the substrate is more biocompatible, the cultured cells will spread on and adhere to the substrate better, and the number of cultured cells will be larger. These will enable the radiobiological effects on the cells to be better observed.

It is established that the biocompatibility of a substrate is dependent on the surface energy (γ_s), and the ratio between its polar component (γ_s^p) to its dispersive component (γ_s^d) (see e.g., Li et al., 2006; Chan et al., 2007). Yang et al. (2002) found that the adhesion of protein is strong when both the dispersive and polar components of the surface tension have similar contributions to the interfacial energy. On the other hand, weak adhesion of protein occurs if only one of the components is dominant in the interfacial energy. Kwok et al. (2004) showed that low values of γ_s^p/γ_s^d indicate preference of protein adhesion. Therefore, surface energy gradient surfaces with changes in the γ_s^p/γ_s^d ratio will be of particular interest for establishing the relationship between the γ_s^p/γ_s^d ratio and the biocompatibility.

To the best of our knowledge, no such gradient surfaces have been fabricated before. The most closely related surfaces that have been fabricated are the wettability gradient surfaces, which are also of interest for establishing the relationship between wettability and biocompatibility. Corona discharge treatment has been proposed to create wettability gradient surfaces (Lee et al., 1992).

In the present paper, we report an innovative method in creating surface energy gradient surfaces on polyallyldiglycol carbonate (CR-39) films through the introduction of latent tracks from alpha-particle irradiation with the fluence increased along the sample length followed by ultraviolet (UV) irradiation. CR-39 films are a kind of solid-sate nuclear track detector (SSNTD). SSNTDs have found wide applications in different branches of science. A most recent review of SSNTDs can be found in Nikezic and Yu (2004).

* Corresponding author: Tel.: +852 2788 7812; fax: +852 2788 7830.
E-mail address: peter.yu@cityu.edu.hk (K.N. Yu).

1350-4487/$ - see front matter © 2008 Elsevier Ltd. All rights reserved.
doi:10.1016/j.radmeas.2008.04.037

2. Methodology

2.1. Sample preparation

The CR-39 SSNTDs used in the present work had a thickness of 100 μm and were purchased from Page Mouldings (Pershore) Limited, Worestershire. The detectors were first cut into films with a size of 2 cm × 5 cm. On each film, we designated five separate regions along the 5 cm side, each having a dimension of 2 cm × 1 cm (see Fig. 1). Different fluence of alpha particles were irradiated onto these five regions (with one region having no alpha-particle irradiation).

For the alpha-particle irradiation, alpha particles with an energy of ~3 MeV were used. The alpha-particle source employed in the present study was a planar ^{241}Am source (main alpha energy = 5.49 MeV under vacuum) with an activity of 0.1 μCi. The energy of the alpha particles was adjusted by changing the source to detector distance under atmospheric pressure. The relationship between the alpha energy and the air distance traveled by an alpha particle with initial energy of 5.49 MeV from ^{241}Am was obtained by measuring the energies for alpha particles passing different distances through normal air using alpha spectroscopy systems (ORTEC Model 5030) with passivated implanted planar silicon (PIPS) detectors of areas of 300 mm^2. The use of a lower alpha energy (such as 3 MeV) implied a larger source to detector distance, which would reduce the differences in the incident angles for the side and center of the detectors.

Along the length of the CR-39 detector, the first region was not irradiated with alpha particles, while the second to the fifth regions were irradiated with the same alpha-particle source and the same source to detector distance for 1, 3, 5 and 7 d, respectively. During alpha-particle irradiation of a particular region, all other regions were covered to prevent alpha-particle irradiation.

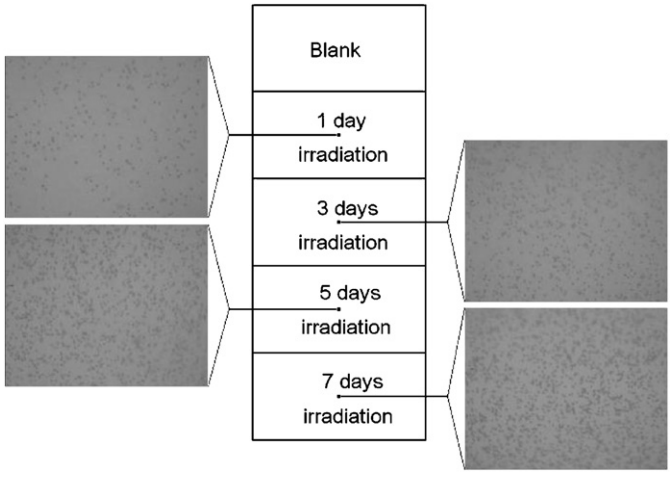

Fig. 1. A CR-39 detector with a size of 2 cm × 5 cm separated into five regions from top to bottom, each having a dimension of 2 cm × 1 cm. The top region was not irradiated with alpha particles, while the second to the fifth regions (from top to bottom) were irradiated with the same alpha-particle source and the same source to detector distance for 1, 3, 5 and 7 d, respectively. The images show the track densities in different regions after chemically etching in aqueous 6.25 N NaOH for 10 min at 70 °C. Different track densities are clearly noticeable in different regions.

After completion of all alpha-particle irradiations, the entire CR-39 detector was irradiated by UV photons with a wavelength of 257 nm from a UVC lamp (model #9815-25, from Cole Palmer) for 13 h. The detectors were then kept inside a plastic container for 2 h before the surface properties were analyzed.

2.2. Surface property analyses

The surface properties of the five different regions on the CR-39 detector were investigated using the sessile drop technique using a contact angle geniometer (JY-82, China). The accuracy of this technique is typically ±2°. The test liquids employed were doubly distilled water, glycerin and ethylene glycol. For water (or liquid phase), the surface tension γ_l, its polar component γ_l^p and its dispersive component γ_l^d are given by $\gamma_l = 72.8$, $\gamma_l^p = 51.0$ and $\gamma_l^d = 21.8\,\mathrm{mJ/m^2}$, respectively. For glycerin, $\gamma_l = 63.4$, $\gamma_l^p = 26.4$ and $\gamma_l^d = 37.0\,\mathrm{mJ/m^2}$. For ethylene glycol, $\gamma_l = 48.3$, $\gamma_l^p = 19.0$ and $\gamma_l^d = 29.3\,\mathrm{mJ/m^2}$. The reported results are the mean of two measurements made on different positions on the same film surface. To avoid cross-contamination, a dedicated microsyringe was used for each liquid.

The work of adhesion (W_a) between a liquid and solid are given by Young (1805) and Eq. (1) and by Van Oss et al. (1988) and Eq. (2):

$$W_a = \gamma_l(1 + \cos\theta) \tag{1}$$

$$W_a = (\gamma_l^p \gamma_s^p)^{1/2} + (\gamma_l^d \gamma_s^d)^{1/2} \tag{2}$$

where θ is the contact angle, γ_s^p and γ_s^d are the polar and dispersive components of the solid phase. From Eqs. (1) and (2), we obtain

$$(\gamma_l^p \gamma_s^p)^{1/2} + (\gamma_l^d \gamma_s^d)^{1/2} = \gamma_l(1 + \cos\theta). \tag{3}$$

In this way, measurements with different liquids with known polar and dispersive components can solve for γ_s^p and γ_s^d.

2.3. Track density analyses

After analyzing the surface properties, the entire CR-39 detector was chemically etched in aqueous 6.25 N NaOH for 10 min at 70 °C to reveal the alpha-particle tracks. These would be used qualitatively for visualization of the track densities in different regions.

3. Results and discussion

The images in Fig. 1 show the track densities in different regions after chemically etching in aqueous 6.25 N NaOH for 10 min at 70 °C. Different track densities are clearly noticeable in different regions.

Table 1 shows the contact angles measured for different regions on the CR-39 detector, namely, UVC only, and 1, 3, 5, 7 d of alpha irradiation +UVC. The contact angles measured for

Table 1
The contact angles (deg) measured for different regions on the CR-39 detector, namely, UVC only, and 1, 3, 5, 7 d of alpha irradiation +UVC

Treatment	Water	Ethylene glycol	Glycerin
Raw	70.6	45.6	68.3
UVC only	70.2	49.7	63.1
1 d alpha irradiation + UVC	71.0	50.7	65.8
3 d alpha irradiation + UVC	71.5	49.1	63.4
5 d alpha irradiation + UVC	71.8	45.7	62.6
7 d alpha irradiation + UVC	76.8	45.7	63.7

The contact angles measured for the raw CR-39 detector (without alpha and UVC irradiations) are also shown for comparison.

Table 2
The surface energy (γ_s), its polar component (γ_s^p), its dispersive component (γ_s^d) and the ratio (γ_s^p/γ_s^d) (all with the unit mJ/m^2) determined for different regions on the CR-39 detector, namely, UVC only, and 1, 3, 5, 7 d of alpha irradiation +UVC

Treatment	γ_s	γ_s^p	γ_s^d	γ_s^p/γ_s^d
Raw	33.0	18.1	14.9	1.22
UVC only	33.6	17.9	15.7	1.14
1 d alpha irradiation + UVC	32.7	18.3	14.4	1.27
3 d alpha irradiation + UVC	33.3	15.9	17.5	0.91
5 d alpha irradiation + UVC	34.3	13.0	20.4	0.64
7 d alpha irradiation + UVC	35.1	8.2	26.9	0.31

The values determined for the raw CR-39 detector (without alpha and without UVC irradiation) are also shown for comparison.

the raw CR-39 detector (without alpha and UVC irradiations) are also shown for comparison. We see that the contact angles do not vary significantly.

Table 2 shows the surface energy (γ_s), its polar component (γ_s^p), its dispersive component (γ_s^d) and the ratio (γ_s^p/γ_s^d) determined for the different regions on the CR-39 detector. Again, the values determined for the raw CR-39 detector are also shown for comparison. Here, we can see that γ_s does not vary significantly with the alpha-particle irradiation. In contrast, γ_s^p decreases steadily (from 18.3 to 8.2 mJ/m^2) while γ_s^d increases steadily (from 14.4 to 26.9 mJ/m^2), and the ratio γ_s^p/γ_s^d decreases significantly (from 1.27 to 0.31) with the alpha-particle fluence.

The underlying mechanism for the changes in surface energies due to alpha-particle irradiation is not clear at this stage. We have studied the chemical changes of the irradiated CR-39 detectors in the present work using FTIR spectroscopy but no apparent changes can be observed. Similarly, Satriano et al. (2000) irradiated surfaces of two polymers, namely, poly-hydroxy-methylsiloxane and polyethylene-terephtalate surfaces, by 5 keV Ar ions. Fluorescence spectroscopy, X-ray photoelectron spectroscopy and contact angle technique were then employed to determine the adsorption kinetics and to characterize the chemical composition and the surface energy of the irradiated surfaces. Their conclusion was that "it was not possible to find a straightforward correlation between irradiation-induced compositional modifications and surface free energy." Further studies will be needed to explain the mechanism for surface-energy changes due to alpha-particle irradiation

In conclusion, we have successfully fabricated a surface energy gradient surface with changes in the γ_s^p/γ_s^d ratio created by latent alpha-particle tracks in the CR-39 SSNTD. These surface energy gradient surfaces will be of particular interest for establishing the relationship between the γ_s^p/γ_s^d ratio and the biocompatibility.

References

Chan, K.F., Ho, J.P.Y., Li, W.Y., Lau, B.M.F., Tse, A.K.W., Fong, W.F., Bilek, M.M.M., McKenzie, D.R., Chu, P.K., Yu, K.N., 2007. Investigation of cytocompatibility of surface-treated cellulose nitrate films by using plasma immersion ion implantation. Surf. Coatings Technol. 201, 6897–6900.

Kwok, S.C.H., Yang, P., Wang, J., Liu, X.Y., Chu, P.K., 2004. Haemocompatibility of nitrogen-doped, hydrogen-free diamond-like carbon prepared by nitrogen plasma immersion ion implantation—deposition. J. Biomed. Mater. Res. A 70, 107–114.

Lee, J.H., Kim, H.G., Khang, G.S., Lee, H.B., Jhon, M.S., 1992. Characterization of wettability gradient surfaces prepared by corona discharge treatment. J. Colloid Interface Sci. 151, 563–579.

Li, W.Y., Chan, K.F., Tse, A.K.W., Fong, W.F., Yu, K.N., 2006. Studies of biocompatibility of chemically etched CR-39 SSNTDs in view of their applications in alpha-particle radiobiological experiments. Nucl. Instrum. Methods Phys. Res. J. B 248, 319–323.

Nikezic, D., Yu, K.N., 2004. Formation and growth of tracks in nuclear track materials. Mater. Sci. Eng. R 46, 51–123.

Satriano, C., Scifo, C., Marletta, G., 2000. Study of albumin adsorption on ion beam irradiated polymer surfaces. Nucl. Instrum. Methods in Phys. Res. B 166-167, 782–787.

Van Oss, C.J., Chanudhury, M.K., Good, R.J., 1988. Interfacial Lifshitz–van der Waals and polar interactions in macroscopic systems. J. Chem. Rev. 88, 927–941.

Yang, P., Huang, N., Leng, Y.X., Chen, J.Y., 2002. Comparative study of blood compatibility between TiO_{2-x} film and LTI-carbon. Chin. J. Biomed. Eng. 21, 90–93.

Young, T., 1805. An essay on the cohesion of fluids. Philos. Trans. R. Soc. 95, 65–87.